

# End-to-end simulation of the C-ADS Injector II with a 3-D field map<sup>\*</sup>

WANG Zhi-Jun(王志军)<sup>1,2,3;1)</sup> HE Yuan(何源)<sup>1,3;2)</sup> WANG Wang-Sheng(王旺生)<sup>1</sup> LIU Shu-Hui(刘淑会)<sup>1</sup>  
 JIA Huan(贾欢)<sup>1</sup> LI Chao(李超)<sup>1,3</sup> XU Xian-Bo(徐显波)<sup>1</sup> CHEN Xi-Meng(陈熙萌)<sup>2</sup>

<sup>1</sup> Institute of Modern Physics, Chinese Academy of Sciences, Lanzhou 73000, China

<sup>2</sup> The School of Nuclear Science and Technology Lanzhou University, Lanzhou 730000, China

<sup>3</sup> University of Chinese Academy of Sciences, Beijing 100049, China

**Abstract:** The Injector II, one of the two parallel injectors of the high-current superconducting proton driver linac for the China Accelerator-Driven System (C-ADS) project, is being designed and constructed by the Institute of Modern Physics. At present, the design work for the injector is almost finished. End-to-end simulation has been carried out using the TRACK multiparticle simulation code to check the match between each acceleration section and the performance of the injector as a whole. Moreover, multiparticle simulations with all kinds of errors and misalignments have been performed to define the requirements of each device. The simulation results indicate that the lattice design is robust. In this paper, the results of end-to-end simulation and error simulation with a 3-D field map are presented.

**Key words:** high-intensity proton linac, end-to-end simulation, 3-D field map, error simulations

**PACS:** 29.27.Bd, 52.65.Rr, 41.20.cv **DOI:** 10.1088/1674-1137/37/4/047003

## 1 Introduction

The China Accelerator-Driven System (C-ADS) [1], which will be an effective tool for transmuting the long-lived transuranic radionuclides produced in nuclear plants into shorter-lived ones, is being studied at the Chinese Academy of Sciences.

The Injector II, as part of the ADS, is being designed and built at the Institute of Modern Physics (IMP). The Injector II is composed of an electron cyclotron resonance (ECR) ion-source, a low-energy beam transport line (LEBT), a radio-frequency quadrupole (RFQ), a medium energy beam transport line (MEBT) and an SC accelerating section. The layout of the Injector II is shown in Fig. 1.

The LEBT will match the proton beam with 0.035 MeV from the ECR source to the RFQ by two solenoids. The RFQ will accelerate and focus the beam from 0.035 MeV to 2.1 MeV, simultaneously. The MEBT

has two main functions, which are to match the proton beam from the RFQ to the superconducting accelerating section and to place some on-line beam diagnostics devices. The superconducting accelerating section will accelerate the proton from 2.1 MeV to 10 MeV with 16 superconducting half wave resonator (HWR) cavities.

The basic parameters of the Injector II are listed in Table 1.

Table 1. The basic parameters of the Injector II.

parameter	value
particle type	proton
operation frequency/MHz	162.5
operation mode	CW
input beam energy/MeV	0.035
output beam energy/MeV	10
beam current/mA	10

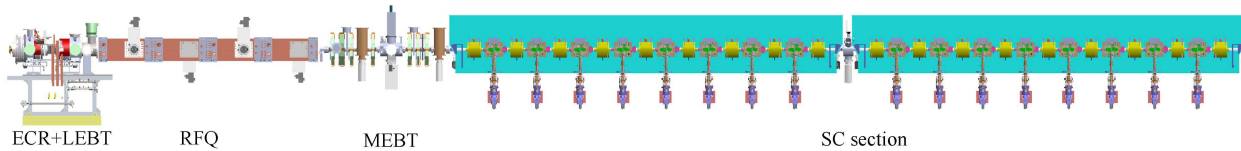


Fig. 1. (color online) The layout of the C-ADS II Injector.

Received 25 May 2012

<sup>\*</sup> Supported by National Natural Science Foundation of China (91026001)

1) E-mail: wangzj@impcas.ac.cn

2) E-mail: hey@impcas.ac.cn

©2013 Chinese Physical Society and the Institute of High Energy Physics of the Chinese Academy of Sciences and the Institute of Modern Physics of the Chinese Academy of Sciences and IOP Publishing Ltd

In this paper, the simulation results of end-to-end simulation and error simulation with a 3-D field map of the HWR cavities and solenoids will be presented.

## 2 The TRACK code

In the TRACK code [2], the transport of a charged particle is described by the motion equation:

$$\frac{d\mathbf{p}}{dt} = q(\mathbf{E} + \mathbf{v} \times \mathbf{B}), \quad (1)$$

where  $\mathbf{p}$  is the momentum of the particle and  $q$  is the charge of the particle.  $\mathbf{E} = \mathbf{E}_{\text{ext}} + \mathbf{E}_{\text{int}}$ , where  $\mathbf{E}_{\text{ext}}$  is the sum of the external electric from acceleration and  $\mathbf{E}_{\text{int}}$  is the internal electric field between particles.  $\mathbf{B} = \mathbf{B}_{\text{ext}} + \mathbf{B}_{\text{int}}$  is the sum of the external magnetic field from focusing elements and the internal magnetic between particles. The external field can be simulated by third party codes, such as Micro Wave Studio [3]. The space charge effect is calculated using particles in the cell method.  $\mathbf{v}$  is the particle velocity. For the trajectory calculation, the fourth order Runge-Kutta method is used. As a Z-code, it uses the independent variable  $z$  to track the phase space coordinates of particles ( $x, x' = dx/dz, y, y' = dy/dz, \beta = v/c, \phi$ ), where  $v = |\mathbf{v}|$  is the amplitude value of velocity, and  $\phi$  is the synchronous phase, which is the particle phase with respect to the RF field at the given section of the accelerator. The transport of the phase space coordinates is shown by the set of equations used for the step-by-step integration calculation:

$$dx/dz = x', \quad dy/dz = y', \quad d\phi/dz = \frac{2\pi f_0 h}{\beta c},$$

$$dx'/dz = \chi \frac{Q}{A} \frac{h}{\beta \gamma} \left[ \frac{h}{\beta c} (E_x - x' E_z) + x' y' B_x - (1 + x'^2) B_y + y' B_z \right],$$

$$dy'/dz = \chi \frac{Q}{A} \frac{h}{\beta \gamma} \left[ \frac{h}{\beta c} (E_y - y' E_z) + x' y' B_x - (1 + y'^2) B_x + x' B_z \right],$$

$$d\beta/dz = \chi \frac{Q}{A} \frac{h}{\beta \gamma^3 c} (E_x x' + x' y' B_x + B_y y' + B_z),$$

where  $\gamma = \frac{1}{\sqrt{1-\beta^2}}$  is the Lorenz factor,  $h = \frac{1}{\sqrt{1+x'^2+y'^2}}$ ,  $\chi = \frac{1}{m_a c^2}$ ,  $A$  is the mass number,  $m_a$  is the atomic unit mass, and  $E_x, E_y, E_z, B_x, B_y, B_z$  are the components of

the electric and magnetic field in each direction in Cartesian coordinates. For more details about the algorithms and functions of TRACK, the manual [4] of the code can be referenced.

## 3 End-to-end simulation of the Injector II

In our case, the end-to-end simulation is carried out for the section from the entrance of the RFQ to the end of the superconducting section. The RFQ is simulated with PARMTEQ-M [5] and the following sections are simulated by TRACK.

### 3.1 The beam dynamics of RFQ

1000000 macro-particles are initialized in a water bag distribution in the transverse direction and a DC beam in the longitudinal direction. The input normalized RMS emittance is 0.30  $\pi\text{mm}\cdot\text{mrad}$  at 35 keV. The beam current is 10 mA. Table 2 shows the main results of the simulation with the PARMTEQ-M code.

Table 2. The main simulation results of RFQ.

parameters	value
transmission (%)	99.7
$\epsilon_x / (\text{mm}\cdot\text{mrad})$	0.3178
$\alpha_x$	0.4602
$\beta_x / (\text{mm}/\text{mrad})$	0.2689
$\epsilon_y / (\text{mm}\cdot\text{mrad})$	0.3155
$\alpha_y$	-0.1042
$\beta_y / (\text{mm}/\text{mrad})$	0.1256
$\epsilon_z / (\text{deg}\cdot\text{MeV})$	0.0571
$\alpha_z$	0.2795
$\beta_z / (\text{deg}/\text{MeV})$	1173.24

In Table 2,  $\epsilon$  is the normalized RMS emittance. The output phase space distribution is plotted in Fig. 2.

### 3.2 The beam dynamics of MEBT and the superconducting section

The MEBT and superconducting section are simulated by the TRACK code. The particles distributed out from the RFQ are transported as the initial distribution of the downstream linac.

The simulation results are shown in Fig. 3. The RMS envelopes in both the transverse and longitudinal direction are smooth and periodic in the superconducting section. This shows that there is good matching between MEBT and the superconducting section.

In the end-to-end simulation, beam loss is not observed in the Injector II. To make sure the beam can be accelerated and transported downstream, the beam emittance evolution in the linac should be analyzed. The emittance growth in each phase space is listed in Table 3.

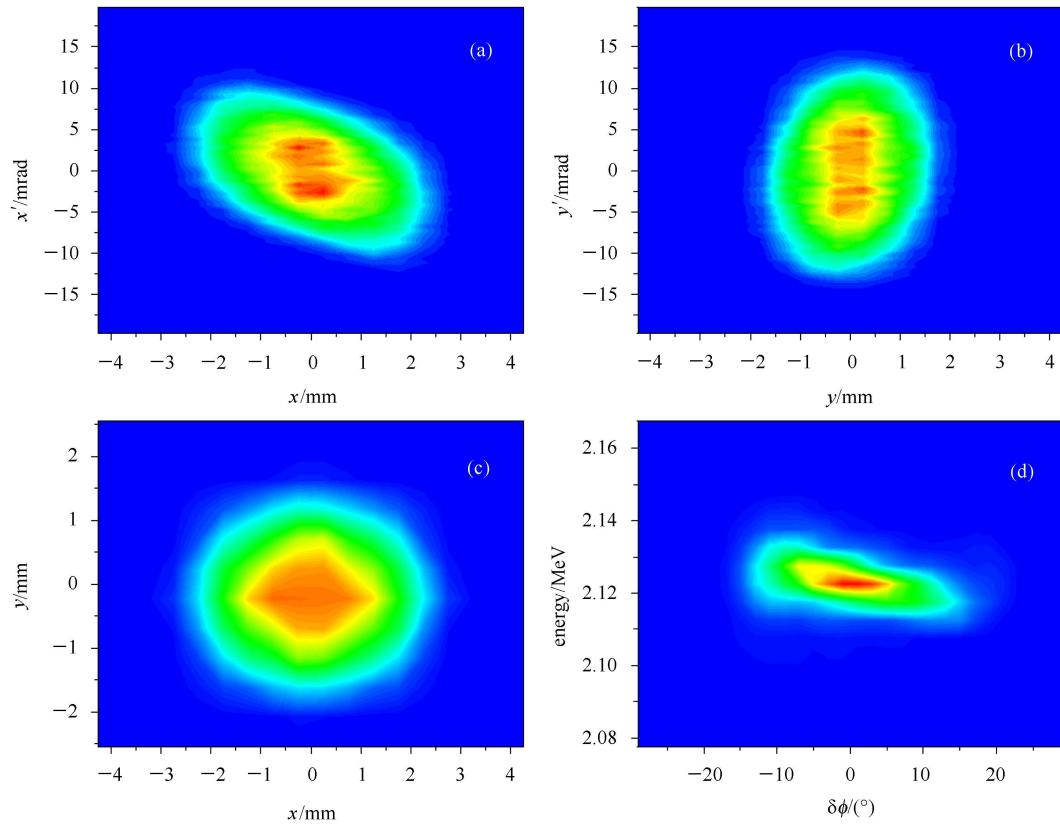


Fig. 2. The output phase distribution of RFQ. (a) is the  $x-x'$  phase space, (b) is the  $y-y'$  phase space, (c) is the  $x-y$  plane, and (d) is the phase space of the longitude.

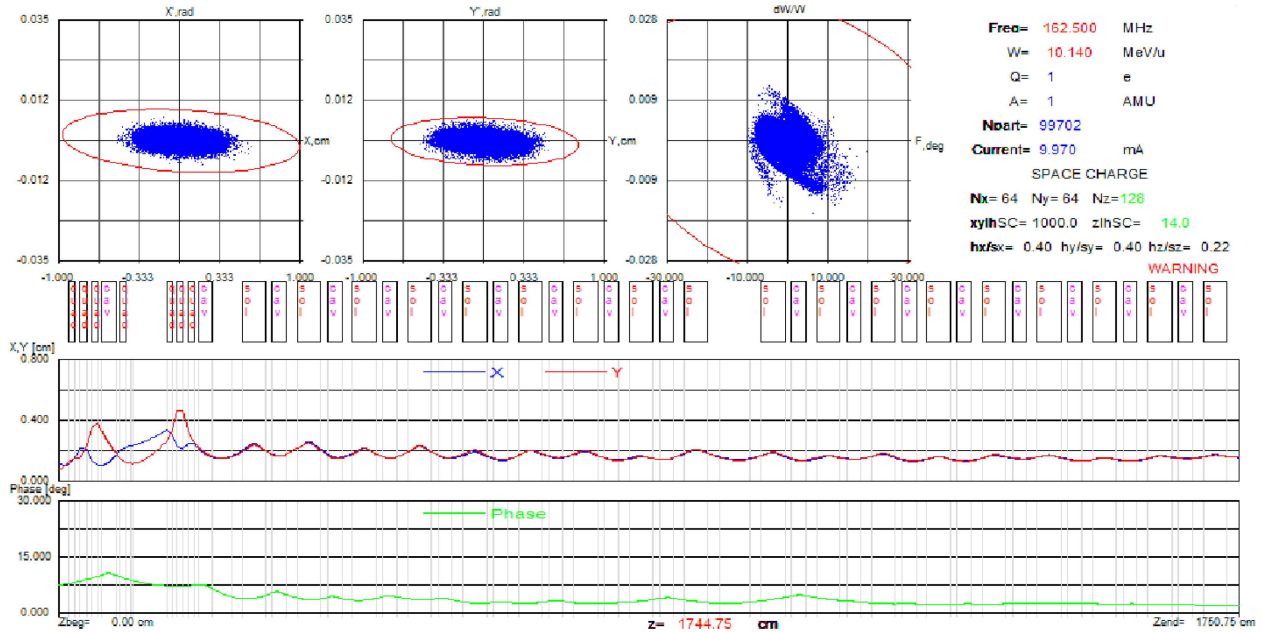


Fig. 3. The simulation results of MEBT and the superconducting section.

In Table 3,  $\epsilon_{0.99}$  is the RMS emittance including 99% particles, and  $\epsilon_{\text{max}}$  is the RMS emittance including all particles. What should be noted is that the longitudinal emittance growth is a comparison with the emittance of the beam extracted from the RFQ, since the emittance at the entrance of RFQ is almost zero.

From Table 3, we can see that the transverse emittance growth is in a reasonable range, while the max longitudinal emittance growth is much larger, even up to 420%. One can also see from the phase space that the longitudinal phase space is distorted and some particles are out of the core. A more detailed simulation of the longitudinal emittance is presented. The emittance growth for the cases of including a different proportion of particles is calculated, and the results are listed in Table 4.

Table 3. The emittance growth in end-to-end simulation.

emittance growth	value
$\epsilon_{x\text{-RMS}}$ (%)	8.33
$\epsilon_{x\text{-}0.99}$ (%)	20.2
$\epsilon_{x\text{-max}}$ (%)	36
$\epsilon_{y\text{-RMS}}$ (%)	8.17
$\epsilon_{y\text{-}0.99}$ (%)	21.3
$\epsilon_{y\text{-max}}$ (%)	33
$\epsilon_{z\text{-RMS}}$ (%)	10
$\epsilon_{z\text{-}0.99}$ (%)	15
$\epsilon_{z\text{-max}}$ (%)	420

We can see from Table 4 that the RMS emittance growth with 0.9999 of particles grows just 20.5%, while the emittance growth with 0.99999 of particles grows 420%, which is the same with max longitudinal emittance growth. This means that one in hundred thousand of the particles are far from the beam core and out of acceleration acceptance. These particles will be lost in the downstream linac. To avoid particle loss in the high energy part, these particles should be collimated at MEBT.

Table 4. The longitudinal emittance growth obtained in end-to-end simulation.

proportion of particles	emittance growth (%)
0.95	23.7
0.99	14.9
0.999	12.6
0.9999	20.5
0.99999	420

### 4 Error simulation of the Injector II

In the TRACK code, the errors and misalignments of the device are described by 10 randomly generated numbers, which stand for the misalignments of an element in six independent coordinates and the static and dynamic errors of the phase and amplitude. For the static error of the phase and the amplitude, the errors are generated

in a uniform distribution between the extreme values  $\pm$  max, and for the dynamic errors they are generated in a Gaussian distribution at  $\pm$  three times the RMS value. The displacement errors are applied to the  $x$  and  $y$  positions of the center of the elements. The rotation errors are applied around the  $z$  axis (beam axis).

For statistical significance, the simulations of each kind of error and misalignment are repeated 200 times, starting from a different seed for the random number generator each time. One million particles are tracked in every simulation. The simulation work is done in parallel on the IMP-linac grid, which include 148 cores.

In the Injector II, there are quadrupoles, bunchers, solenoids and superconducting cavities. All devices with all kinds of errors are simulated to produce the allowable error and misalignments range listed in Table 5. The goal is that the maximum envelope in the transverse direction is about 75% of the aperture.

Table 5. Error and misalignment value distribution.

	quadrupole	buncher	solenoid	SC cavity
$\delta x/\text{mm}$	$\pm 0.2$	$\pm 0.5$	$\pm 0.75$	$\pm 1.0$
$\delta y/\text{mm}$	$\pm 0.2$	$\pm 0.5$	$\pm 0.75$	$\pm 1.0$
$\delta z/\text{mm}$	$\pm 1.0$	$\pm 1.0$	$\pm 1.0$	$\pm 1.0$
$\theta x/\text{mrad}$	$\pm 5.0$	$\pm 5.0$	$\pm 2.5$	$\pm 5.0$
$\theta y/\text{mrad}$	$\pm 5.0$	$\pm 5.0$	$\pm 2.5$	$\pm 5.0$
$\theta z/\text{mrad}$	$\pm 3$	$\pm 5.0$		
$\delta\phi_j/(\text{^\circ})$		$\pm 0.5$		$\pm 0.5$
$\delta F_j$ (%)	$\pm 0.05$	$\pm 0.5$	$\pm 0.05$	$\pm 0.5$
$\delta\phi_s/(\text{^\circ})$		$\pm 1.0$		$\pm 1.0$
$\delta F_s$ (%)	$\pm 0.01$	$\pm 1.0$	$\pm 0.01$	$\pm 1.0$

As shown in Table 5,  $\delta\phi_j$  and  $\delta F_j$  are the RMS dynamic errors of the phase and amplitude of the field, and  $\delta\phi_s$  and  $\delta F_s$  are the static errors of the phase and amplitude of the field. From Table 5, we can see that the quadrupoles are sensitive to the transverse displacement, while the solenoid errors from the tilt are more crucial.

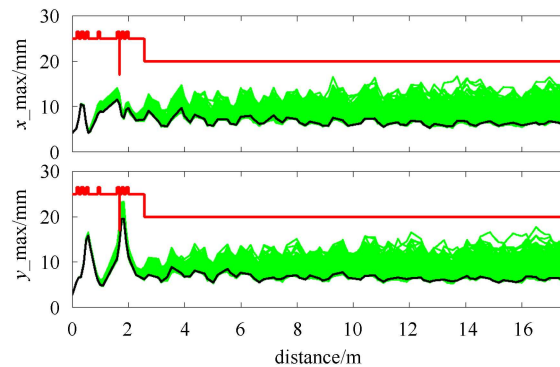


Fig. 4. The maximum envelope along  $z$  with errors and misalignments. The red line is the aperture of the device, and the plots show in solid green the superposition of the results from 400 sets of errors. The black curves correspond to the reference case with no errors.

The maximum envelope along  $z$  with errors and misalignments is shown in Fig. 4. The aperture is 50 mm in MEBT and 40 mm in the superconducting section. A collimator is placed in MEBT to scrape off the particles far from the beam core transversely. The maximum envelope is about 15 mm, which is 75% of the aperture in the superconducting section.

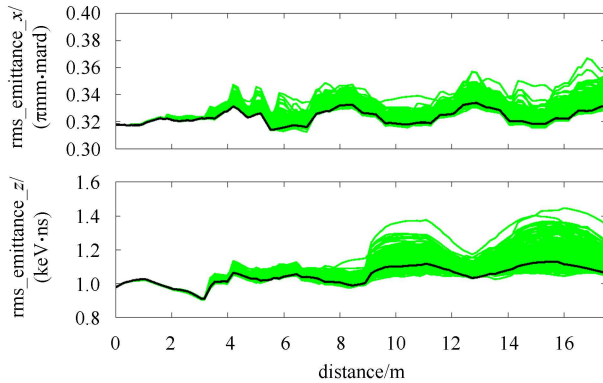


Fig. 5. The emittance, which varies along  $z$  with errors and misalignments. The plots show in solid green the superposition of the results from 400 sets of errors, and the black line is the ideal case.

The emittance variation along  $z$  with errors and misalignments is shown in Fig. 5. The transverse and longitudinal RMS emittance, which evolve along  $z$ , are plotted. Under the errors and misalignments value, the final emittance growth is 15% in the transverse and 40% in the longitudinal. The final emittances with errors are far lower than the acceptance of the downstream linac.

## 5 Summary

In this paper, end-to-end simulation is presented. Multiparticle simulation with the TRACK code shows that there is a good match between every conjoined accelerating section, and that the whole linac has good performance. The emittance growth in both the transverse and longitudinal direction is in a reasonable range, and the error simulation results indicate that the lattice is robust and not sensitive to errors. More detailed beam loss analysis will be performed next.

*Zhijun Wang would like to express his sincere thanks to Brahim Mustapha (ANL) for his kind help in using the TRACK code and for useful discussions about the error simulation analysis, and Yang Qiong (IMP) for her hard work in building the IMP-linac grid.*

## References

- 1 WANG Zhi-Jun, HE Yuan, LIU Yong et al. Chinese Physics C, 2012, **36**(3): 256–260
- 2 Aseev V N, Ostroumov P N, Lessner E S et al. Proceedings of 2005 Particle Accelerator Conference. Knoxville, Tennessee, 2053-2055, 2005. <http://cdsweb.cern.ch/record/927002>
- 3 <http://www.cst.com/Content/Products/MWS/Overview.aspx>. A Specialist Tool for the 3D EM Simulation of High Frequency Components, 2011
- 4 Ostroumov P N, Aseev V N, Mustapha B. TRACK-a Code for Beam Dynamics Simulation in Accelerators and Transport Lines with 3D Electric and Magnetic Fields. 2007. [http://www.phy.anl.gov/atlas/TRACK/Trackv37/Manuals/tv37\\_man\\_index.html](http://www.phy.anl.gov/atlas/TRACK/Trackv37/Manuals/tv37_man_index.html) Accelerator Conf, Oregon, USA, 11-15, 2003. <http://accelconf.web.cern.ch/AccelConf/p03/PAPERS/MOAL003.pdf>
- 5 Crandall K R et al. RFQ Design Codes, LA-UR-96-1836. Los Alamos National Laboratory. 1997